Obliquely propagating ion acoustic solitary waves in a dusty plasma in the presence of an external magnetic field

Sarit Maitra and Rajkumar Roychoudhury
Physics and Applied Mathematics Unit, Indian Statistical Institute, Kolkata 700108, India

The obliquely propagating nonlinear ion acoustic wave in a dusty plasma subjected to an external magnetic field is studied in the Sagdeev's pseudopotential framework. The Sagdeev's potential is derived in two cases, one of which assumes the quasineutrality condition and the other uses the Poisson equation instead. The respective ranges of parameters for which solitary waves exist in both the cases are studied in some detail numerically.

I. INTRODUCTION

Dusty plasma can be defined as a plasma with highly charged and extremely massive dust grains. It occurs in various astrophysical as well as laboratory environments.[1] Different types of wave phenomenon in dusty plasma have been studied extensively.[1–12]

The presence of the highly charged and massive dust grains in a plasma introduces new eigenmodes. They are, for example, dust acoustic mode,[2] dust ion-acoustic mode,[3] dust-lower hybrid mode,[4] dust drift mode,[5] etc. Experimental observations on dust acoustic waves and dust ion acoustic waves have been reported by Barkan *et al.*, Thompson *et al.*,[7] and Nakamura *et al.*[8] Several authors[9–12] have studied waves in dusty plasma in the presence of a magnetic field. Electrostatic modes in a magnetized dusty plasma have also been studied by some authors.[13,14] Choi *et al.*[15,16] have studied the nonlinear ion acoustic solitary wave in a magnetized dusty plasma, obliquely propagating to an external magnetic field in the framework of the Sagdeev potential.[17] They have reported that when the ion charge density is high, the Sagdeev potential needs to be expanded up to δn^4 near $n=1$. They also found that rarefactive ion acoustic solitary waves as well as the kink-type double layer solutions could exist, in addition to that conventional hump-type ones found in the δn^3 expansion. Choi *et al.*[15] used the charge neutrality condition, which is valid when the length scale L of the solitary wave is greater than the Debye length λ_D or gyroradius r_g, to derive the pseudopotential for the ion acoustic solitary wave in a dusty plasma. Mamun *et al.*[18] investigated obliquely propagating electron-acoustic solitary waves in a magnetized plasma with two temperature electrons and ions where the hot electrons follow a vortex-like distribution. They obtained a modified Korteweg-de Vries (KdV) equation and derived its stationary solitary solution. We consider a plasma comprising, apart from the ions and Boltzmann distributed electrons, massive dust grains. The magnetic field ($\mathbf{B}$) is taken along the z axis, so that $\mathbf{B}=B_0\mathbf{e}_z$. The dust dynamics is not taken into account and the charge of the dust grains are assumed to be constant. Our work differs from the one by Choi *et al.*[15] in the sense that we have not assumed the charge neutrality condition, which means the parameter β, to be explained later, cannot be taken too large. It may be mentioned that the charge neutrality condition should be critically examined, particularly in the case of double layers where the potential drop can be large enough to accelerate the ions. Also we have derived the exact Sagdeev's potential in the quasineutral case and found some discrepancies in the result given in Ref. 15. However, like Choi *et al.*,[15] we assume that the ion mass alone provides the inertia and the massless electrons follow the Boltzmann relation and the ion temperature is considered to be small compared to that of the electron. In fact the ion temperature is neglected in this study. Experimental and theoretical investigations of waves in a plasma with hot electrons as well as cold ions have been done by several authors.[18] For example, as in a cold plasma, where the ion temperature is near that of ambient, the electron temperature may be of several thousand degrees. The organization of the paper is as follows. In Sec. II the basic equations governing the plasma system are given. Also the Sagdeev's potential for this system is derived here. Discussion of the results and the conclusion are mentioned in Sec. III.

II. BASIC EQUATIONS FOR DIFFERENT SPECIES

The basic equations for ions are

$$\frac{\partial n_i}{\partial t} + \nabla \cdot (n_i \mathbf{v}_i) = 0, \tag{1}$$

$$\frac{\partial \mathbf{v}_i}{\partial t} + (\mathbf{v}_i \cdot \nabla)\mathbf{v}_i = -\frac{e \nabla \phi}{m_i} + \frac{eB_0}{m_i c}\mathbf{v}_i \times \mathbf{e}_z, \tag{2}$$

$$\nabla^2 \phi = -4\pi[-en_e + en_i - ez_d n_d], \tag{3}$$

where n_s ($s=i,e,d$) are the number density of the sth species. Here i,e,d stand for ion, electron, and dust grain, respectively. v_i, m_i are, respectively, the velocity and mass of the ions. Here ϕ is the plasma potential and z_d represents the dust charge number so that charge of the dust is given by $q_d=-ez_d$, where e is the elementary charge. The density of the electrons is given by

$$n_e = n_{e0} \exp\left(\frac{e\phi}{T_e}\right). \tag{4}$$

We assume that the wave is propagating in the x-z plane. After normalization the system reduces to

$$\frac{\partial n}{\partial t} + \frac{\partial}{\partial x}(nv_x) + \frac{\partial}{\partial z}(nv_z) = 0, \tag{5}$$

$$\frac{\partial v_x}{\partial t} + \left(v_x\frac{\partial}{\partial x} + v_z\frac{\partial}{\partial z}\right)v_x = -\frac{\partial \phi}{\partial x} + v_y, \tag{6}$$

$$\frac{\partial v_y}{\partial t} + \left(v_x\frac{\partial}{\partial x} + v_z\frac{\partial}{\partial z}\right)v_y = -v_x, \tag{7}$$

$$\frac{\partial v_z}{\partial t} + \left(v_x\frac{\partial}{\partial x} + v_z\frac{\partial}{\partial z}\right)v_z = -\frac{\partial \phi}{\partial z}, \tag{8}$$

$$\left(\frac{\partial^2}{\partial x^2} + \frac{\partial^2}{\partial z^2}\right)\phi = \beta[\exp \phi - \delta_1 n + \delta_2], \tag{9}$$

where $\beta = r_g^2/\lambda_e^2$, $\delta_1 = n_{i0}/n_{e0}$, $\delta_2 = n_d z_d/n_{e0}$. $r_g = C_s/\Omega$ is the ion gyroradius and $\lambda_e = (T_e/4\pi n_{e0}e^2)^{1/2}$ is the electron Debye length.

The normalizations are $\Omega t \to t$, $(C_s/\Omega)\nabla \to \nabla$, $v_i/C_s \to v$, $n_i/n_{i0} \to n$, $e\phi/T_e \to \phi$, where $C_s = (T_e/m_i)^{1/2}$ is the ion acoustic velocity, $\Omega = eB_0/m_i c$ is the ion gyrofrequency. n_{e0}, n_{i0} are the electron and ion densities, respectively, in the unperturbed state. It can be seen that when r_g is small, β cannot be assumed to be too large and hence *a priori* charge neutrality condition cannot be assumed. To obtain the dispersion relation for low frequency waves we write the dependent variables as the sum of the equilibrium and perturbed parts. We put $n = 1 + \bar{n}$, $v_x = \bar{v}_x$, $v_z = \bar{v}_z$, $\phi = \bar{\phi}$, $v_y = \bar{v}_y$. Equations (5)–(9) can be written as

$$\frac{\partial \bar{n}}{\partial t} + \frac{\partial \bar{v}_x}{\partial x} + \frac{\partial \bar{v}_z}{\partial z} = 0, \tag{10}$$

$$\frac{\partial \bar{v}_x}{\partial t} = -\frac{\partial \bar{\phi}}{\partial x} + \bar{v}_y, \tag{11}$$

$$\frac{\partial \bar{v}_y}{\partial t} = -\bar{v}_x, \tag{12}$$

$$\frac{\partial \bar{v}_z}{\partial t} = -\frac{\partial \bar{\phi}}{\partial z}, \tag{13}$$

$$\left(\frac{\partial^2}{\partial x^2} + \frac{\partial^2}{\partial z^2}\right)\bar{\phi} = \beta[\bar{\phi} - \delta_1 \bar{n}]. \tag{14}$$

We assume the perturbation is of the form $\exp i(k_x x + k_z z - \omega t)$, where k_x, k_z are the wave numbers in the x and z directions, respectively, and ω is the wave frequency. The dispersion relation for the low frequency ($\omega \ll \Omega$) ion acoustic wave is obtained as

$$\omega = k_z\left[\frac{1}{\delta_1} + k_x^2\left(-1 + \frac{1}{\beta\delta_1}\right) + \frac{k_z^2}{\beta\delta_1}\right]^{-1/2} \tag{15}$$

In order to have a travelling wave solution of the system of Eqs. (5)–(9) we introduce a new variable

$$\xi = l_x x + l_z z - Mt, \tag{16}$$

where l_x, l_z are directional cosines and M is the Mach number of the localized wave. Equations (5)–(9) can then be reduced to ordinary differential equations in terms of ξ,

$$M(1-n) + (l_x v_x + l_z v_z)n = 0, \tag{17}$$

$$-M\frac{dv_x}{d\xi} + \left(l_x v_x\frac{d}{d\xi} + l_z v_z\frac{d}{d\xi}\right)v_x = -l_x\frac{d\phi}{d\xi} + v_y, \tag{18}$$

$$-M\frac{dv_y}{d\xi} + \left(l_x v_x\frac{d}{d\xi} + l_z v_z\frac{d}{d\xi}\right)v_y = -v_x, \tag{19}$$

$$-M\frac{dv_z}{d\xi} + \left(l_x v_x\frac{d}{d\xi} + l_z v_z\frac{d}{d\xi}\right)v_z = -l_z\frac{d\phi}{d\xi}, \tag{20}$$

$$(l_x^2 + l_z^2)\frac{d^2\phi}{d\xi^2} = \beta[e^{\phi} - \delta_1 n + \delta_2]. \tag{21}$$

From (18) and (17),

$$\frac{M}{n}\frac{dv_x}{d\xi} = l_x\frac{d\phi}{d\xi} - v_y, \tag{22}$$

and from (19) and (17)

$$\frac{M}{n}\frac{dv_y}{d\xi} = v_x. \tag{23}$$

From (20) and (17),

$$\frac{M}{n}\frac{dv_z}{d\xi} = l_z\frac{d\phi}{d\xi}. \tag{24}$$

Let

$$F(\phi) = \int_0^{\phi} n\, d\phi, \tag{25}$$

then

$$v_z = \frac{l_z}{M}F(\phi). \tag{26}$$

From (26), (25), and (17)

$$l_x v_x + \frac{l_z^2}{M}F(\phi) = \left[1 - \frac{1}{F'(\phi)}\right]M, \tag{27}$$

and from (21)

$$(l_x^2 + l_z^2)\frac{1}{2}\left(\frac{d\phi}{d\xi}\right)^2 = \beta[e^{\phi} - 1 - \delta_1 F(\phi) + \delta_2\phi]. \tag{28}$$

As we can see, Eq. (21) can be integrated to the form $\frac{1}{2}(d\phi/d\xi)^2 + \psi(\phi) = 0$. The equation can be interpreted as an "energy integral" of an oscillatory particle of an unit mass with velocity $d\phi/d\xi$ and position ϕ in a potential well $\psi(\phi)$.

This is the reason for $\psi(\phi)$ to be called a pseudopotential or sometimes referred to as Sagdeev's potential.[17]

It is seen that $\psi(\phi)=0$, $d\psi/d\phi=0$ at $\phi=0$. Hence solitary wave solutions exist if

(i) $d^2\psi/d\phi^2<0$, at $\phi=0$;

(ii) there exists a nonzero ϕ_m, the maximum (or, minimum) value of ϕ, at which $\psi(\phi_m)=0$;

(iii) $\psi(\phi)<0$, when ϕ lies between 0 and ϕ_m.

From (22), (23), (27), and (28) one can get an equation in $F(\phi)$, which when solved would give $F(\phi)$ in terms of ϕ. However, in case of a small amplitude $F(\phi)$ is expanded in terms of ϕ given as,

$$F(\phi)=\phi+a_1\phi^2+a_2\phi^3+a_3\phi^4+a_4\phi^5+\cdots \tag{29}$$

From (27),

$$v_x=A\phi+B\phi^2+C\phi^3+D\phi^4. \tag{30}$$

The values of A, B, C, D are given in the Appendix. From (28),

$$\left(\frac{d\phi}{d\xi}\right)^2=\frac{\beta}{l_x^2+l_z^2}\left[\phi^2(1-2\delta_1a_1)+\phi^3\left(\frac{1}{3}-2\delta_1a_2\right)+\phi^4\left(\frac{1}{12}-2\delta_1a_3\right)\right]. \tag{31}$$

Keeping terms up to ϕ^2,

$$\frac{d^2\phi}{d\xi^2}=A_1\phi+A_2\phi^2=-\frac{d\psi}{d\phi}, \tag{32}$$

where,

$$A_1=\frac{\beta}{l_x^2+l_z^2}(1-2\delta_1a_1),\quad A_2=\frac{\beta}{l_x^2+l_z^2}\left(\frac{1}{2}-3\delta_1a_2\right). \tag{33}$$

From (23),

$$M\frac{d\phi}{d\xi}\frac{dv_y}{d\phi}=v_xF'(\phi), \tag{34}$$

and from (22)

$$v_y=\left[l_x-\frac{M}{F'(\phi)}\frac{dv_x}{d\phi}\right]\frac{d\phi}{d\xi}. \tag{35}$$

From (35) and (34), equating equal powers of ϕ, a_1, a_2 are determined from the equations

$$A=Y_1(1-2\delta_1a_1), \tag{36}$$

$$a_2\left[\frac{3M}{l_x}X_2+3Y_1\delta_1\right]=Z_1X_2-2Aa_1+X_1(1-2\delta_1a_1)Aa_1+\frac{Y_1}{2}. \tag{37}$$

The expressions for X_1, X_2, Y_1, Z_1 are given in the Appendix. Integrating Eq. (32),

$$\phi=-\frac{3(1-2\delta_1a_1)}{1-6\delta_1a_2}\,\mathrm{sech}^2\left(\frac{\sqrt{A_1}\xi}{2}\right). \tag{38}$$

Keeping terms up to ϕ^3,

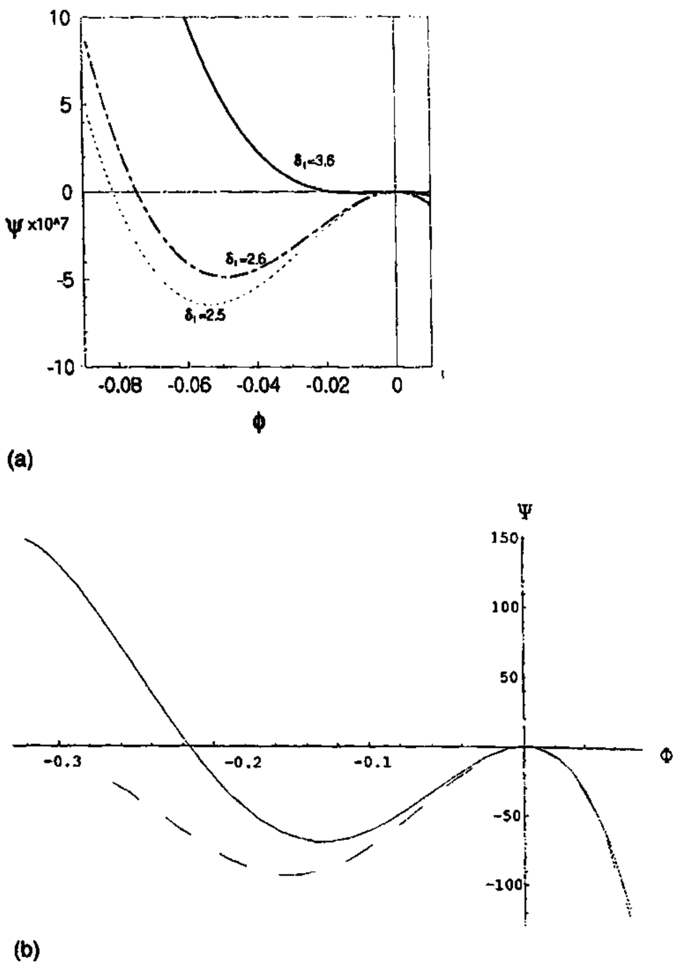

FIG. 1. (a) Sagdeev's potential $\Psi=\psi*10^7$ vs ϕ is plotted, where the dust plasma parameters are $\beta=0.48$, $M=0.2$, $l_z=0.1$, $l_x=\sqrt{1-l_z^2}$. The values of δ_1 are $\delta_1=2.5,2.6,3.6$. Here the solid curve corresponds to $\delta_1=3.6$ and the middle and lower dotted curves represent the cases $\delta_1=2.6$ and $\delta_1=2.5$, respectively. (b) Sagdeev's potential $\Psi=\psi*10^7$ is plotted against ϕ where $\beta=0.75,0.78$. Here $M=0.2$, $l_z=0.1$, and $\delta=2.6$. $\beta=0.75$ corresponds to the solid curve and the dotted curve is plotted for $\beta=0.78$.

$$\frac{d^2\phi}{d\xi^2}=A_1\phi+A_2\phi^2+A_3\phi^3, \tag{39}$$

where

$$A_3=\frac{\beta}{l_x^2+l_z^2}\left(\frac{1}{6}-4\delta_1a_3\right), \tag{40}$$

and a_3 is determined from the equation

$$a_3\left[\frac{4M}{l_x}+\frac{9X_1(1-2\delta_1a_1)M}{l_x}+4Y_1\delta_1\right]=\frac{X_1}{4}(1-2\delta_1a_1)\times[C-4Ba_1+A(4a_1^2-3a_2)]+X_3, \tag{41}$$

where X_3 is given in the Appendix. Integrating Eq. (39),

$$\phi=\left[-\frac{A_2}{3A_1}-\sqrt{\frac{A_2^2}{9A_1^2}-\frac{A_3}{2A_1}}\cosh(\sqrt{A_1}\xi)\right]^{-1}. \tag{42}$$

If $A_2^2=\frac{9}{2}A_1A_3$, then solution (42) would not be valid and a shock wave solution is obtained which is given by

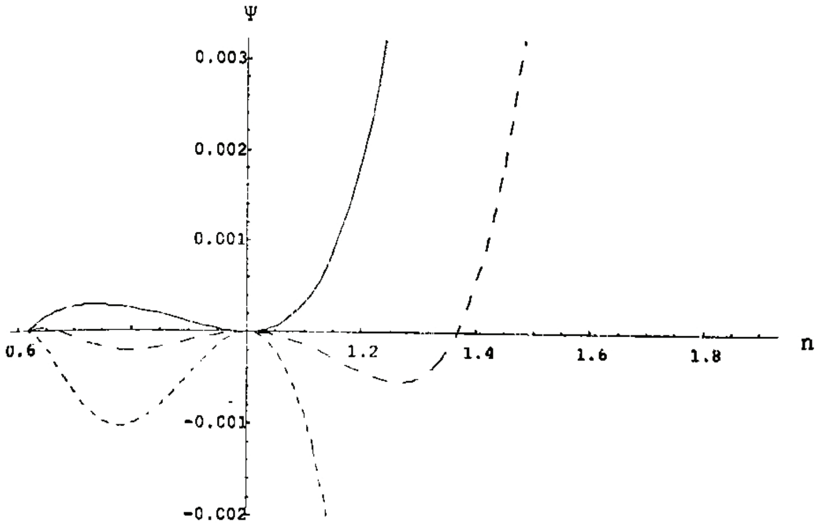

FIG. 2. Sagdeev's potential $\psi(\phi)$ vs n is plotted assuming quasineutrality where the parameters are $\delta_1=2.6$, and $l_z=0.1, 0.11, 0.13$; other parameters are the same as Fig. 1. Here the solid curve corresponds to $l_z=0.13$. The middle dotted curve is for $l_z=0.11$ and the lower curve is for $l_z=0.1$.

$$\phi=-\frac{3A_1}{2A_2}(1+\tanh\alpha(\xi+\xi_0)), \tag{43}$$

where ξ_0 is an integration constant and

$$\alpha=-\frac{A_2}{3\sqrt{2A_3}} \quad (A_3>0). \tag{44}$$

To compare our result with that of Ref. 15 we derive the Sagdeev potential assuming charge neutrality condition, viz., $e^{\phi}=\delta_1 n-\delta_2$, we have,

$$\psi(\phi)=\frac{1}{(n-N_d)^2}\frac{\left(\frac{l_z}{M}\right)^2\psi_1(\phi)+\psi_2(\phi)}{\left[-\frac{M^2}{n^3}+\frac{1}{n-N_d}\right]^2}, \tag{45}$$

where

$$N_d=\frac{\delta_2}{\delta_1} \tag{46}$$

and

$$\psi_1(\phi)=N_d\left\{(n-1)+\frac{N_d}{2}\ln\frac{n-N_d}{1-N_d}\right\}\ln\frac{n-N_d}{1-N_d}+\frac{(n-1)^2}{2} -M^2\left\{\ln n+\frac{1-n}{n}\right\}, \tag{47}$$

$$\psi_2(\phi)=\left[1-N_d-l_z^2\frac{n-N_d}{n}\right]\ln\frac{n-N_d}{1-N_d}+l_z^2\ln n-n+1 -M^2\left(\frac{1}{n}-\frac{1}{2n^2}\right)+\frac{M^2}{2}. \tag{48}$$

Note that the terms connected to the M^2 term in (48) were omitted in Ref. 15. This will affect the numerical evaluation of the Sagdeev's potential as well. To study double layers we expand $\psi(n)$ in terms of n we have

$$\psi(n)=A\delta n^2+B\delta n^3+C\delta n^4, \tag{49}$$

where

$$A=\frac{1}{2}\cdot\frac{M^2(N_d-1)+l_z^2}{M^2A_1}+\frac{M^2}{2A_1^2}(1-N_d)^2, \tag{50}$$

$$B=\frac{1}{6}\cdot\frac{B_1}{(N_d-1)M^2A_1^2}+\frac{M^2}{2A_1^2}\left[(1-N_d)(6-N_d) -2(3-M^2)\frac{(1-N_d)^2}{A_1}\right], \tag{51}$$

$$C=\frac{1}{24}\cdot\frac{C_1}{(N_d-1)^2M^2A_1^3}+\frac{M^2}{2A_1^2}\left[15-20N_d+6N_d^2 -\frac{2(3-M^2)(1-N_d)(6-N_d)}{A_1}\right]+C_2, \tag{52}$$

where $C_2=(3-M^2)^2(1-N_d)^2/A_1^2$; A_1, B_1, C_1 are the same as mentioned in Ref. 15. For double layers to exist $\psi(n)$ should have a double root at $\phi=0$ and a nonzero $\phi=\phi_m$. The condition for double root of the polynomial on the right-hand side of Eq. (49) is

$$B^2=4AC. \tag{53}$$

This condition imposes a constraint among the parameters. If we keep other parameters fixed then we get a relation between M and l_z. When M is plotted against l_z it can be seen that this relation is different from the one in Ref. 15.

III. DISCUSSION AND CONCLUSION

Before going into detail let us first observe that Eqs. (38) and (42) would not be valid for $\delta_1 a_1=\frac{1}{2}$ or $\delta_1 a_2=\frac{1}{6}$. In these cases one needs a higher order term to obtain solitary waves. Also when $A_1<0$, only oscillatory solutions would be obtained. So to obtain solitary waves it is assumed that $A_1>0$ and $A_3\neq 0$. In Fig. 1 $\psi*10^7$ is plotted against ϕ, taking terms up to ϕ^4 [Eq. (31)] when $\beta=0.479$, $l_z=0.1$ and $\delta_1=2.5$, 2.6, and 3.6. It is seen that with increasing δ_1 the wave amplitude decreases. This agrees with results from Choi *et al.*[15] $\delta_1=3.6$ is the critical value beyond which solitary waves would not exist. It is also seen that only a compressive-type solution is obtained. In Fig. 1(a) $\psi*10^7$ is plotted against ϕ

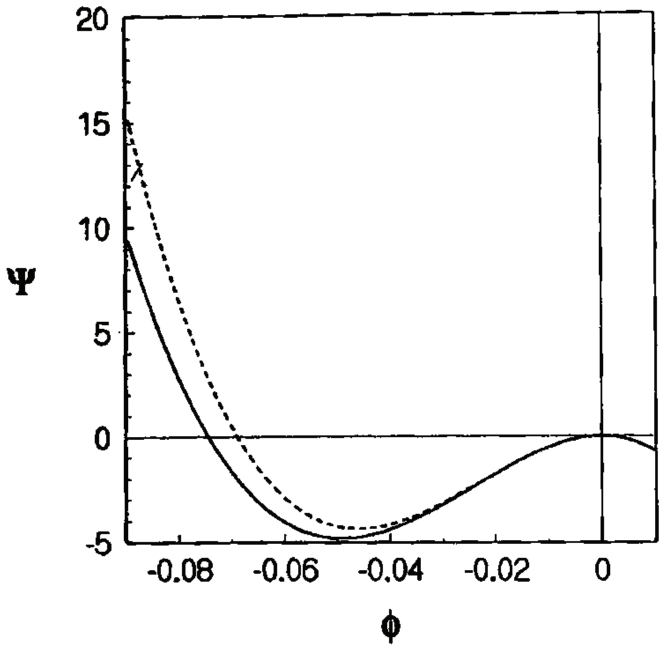

FIG. 3. Sagdeev's potential $\Psi=\psi*10^7$ vs ϕ is plotted taking terms up to ϕ^4 and ϕ^3. The dotted curve represents the lower order and the solid curve corresponds to the higher order case. Here $\delta_1=2.6$ and the value of the other parameters are the same as those in Fig. 1.

for $\delta=2.6$ and $\beta=0.75, 0.78$. $\beta=0.79$ is the critical value of β, for this value of δ, beyond which solitons will not exist.

In Fig. 2 the exact Sagdeev's potential is plotted against the ion density n in the quasineutral case. Here $\delta_1=2.6$ and three values of l_z are used. The values of other parameters are same as Fig. 1. It is seen that for $l_z=0.1$ only rarefactive solitary waves exist, whereas for $l_z=0.11$ both compressive and rarefactive solitary waves coexist. For $l_z=0.13$ solitary waves do not exist. In Fig. 3, $\Psi(\phi)$ is plotted taking terms up to ϕ^3 and ϕ^4. It is found that inclusion of higher order term brings small changes in the amplitude of the soliton, though the nature and shape of $\Psi(\phi)$ remain the same. From Fig. 4, we find that the amplitude of the sech (Ref. 2) solution given by (38) with respect to the variation of δ_1 remains negative. Figure 5 shows the range of parameters in the quasineutral

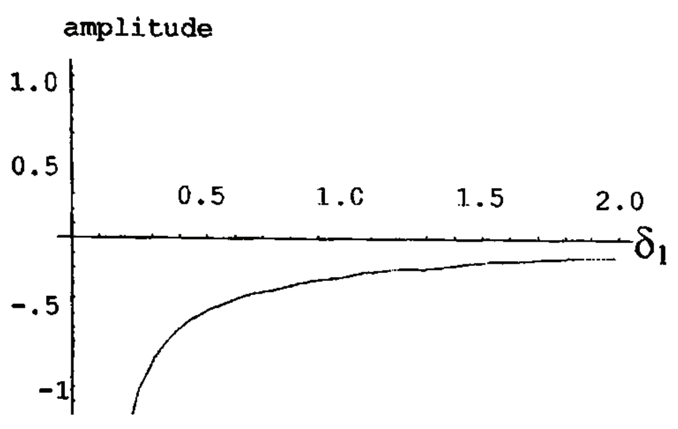

FIG. 4. The amplitude of the solitary wave given by expression (38) has been plotted against δ_1 without using quasineutrality. The value of the dust plasma parameters are $\beta=0.479$, $l_z=0.1$, $M=0.2$; other parameters are the same as those in Fig. 1.

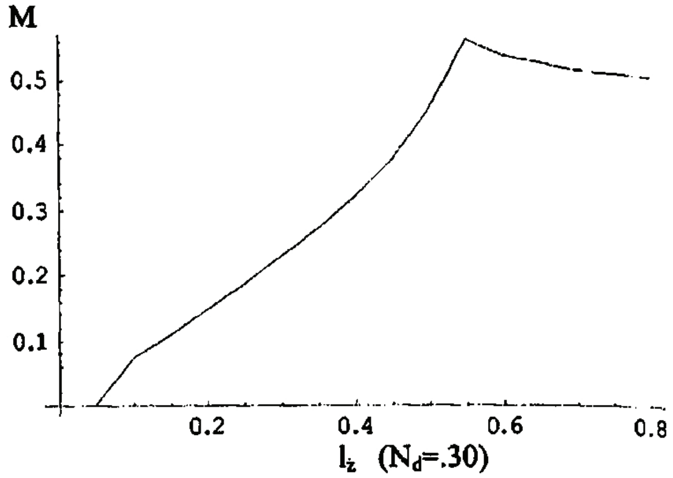

FIG. 5. M vs l_z is plotted in the quasineutral case showing the region of existence of the double layer. The relation between M and l_z is obtained from the condition given in Eq. (53).

case for which double layers will exist. Here M against l_z is plotted when $N_d=0.3$. As mentioned earlier this relation is different from the one given in Ref. 15 [Fig. 6(b) of Ref. 15]. In Fig. 6, the dotted curve shows the potential profile against ξ using the relation (38) and the solid curve corresponds to the same when the relation (42) is used. $\psi*10^7$ vs ϕ is plotted in Fig. 7 with $\delta_1=2.5$, $M=0.2$, $l_z=0.1$ for two values of β, viz., $\beta=0.3$ and 0.4. Here the solid curve is for $\beta=0.3$ and the dotted curve is for $\beta=0.4$. It is seen that the amplitude of the solitary wave increases with β. To get a realistic picture we use β from Ref. 19. Figure 8 shows that as l_z decreases the amplitude decreases which agrees with results from Ref. 15. In Fig. 9 we plot $\psi*10^6$ for the case when $A_1<0, A_2^2$

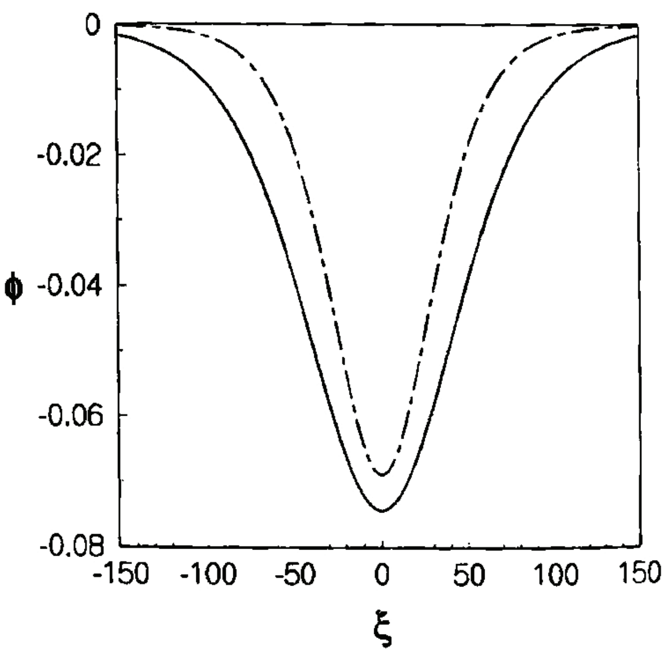

FIG. 6. ϕ vs ξ is plotted using the expressions (42) and (38) with $\delta_1=2.6$, where other parameters are the same as those used in Fig. 1. The dotted curve corresponds to the lower order and the solid curve is for the higher order case.

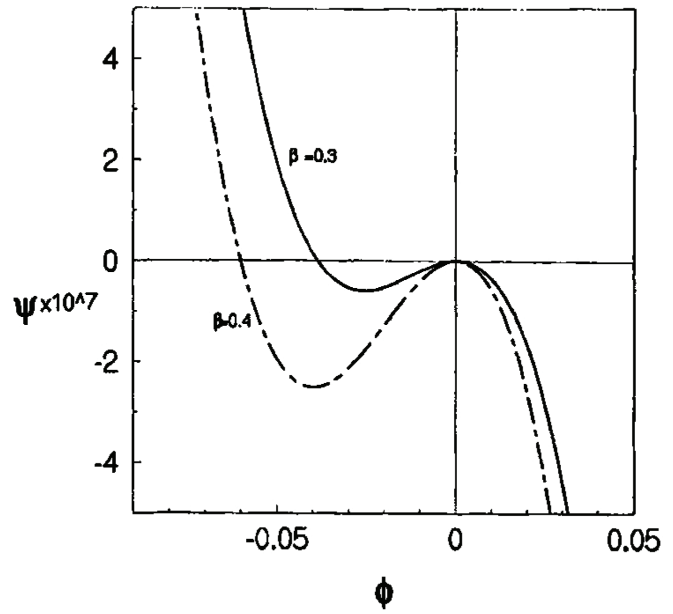

FIG. 7. Sagdeev's potential $\Psi=\psi*10^7$ vs ϕ is plotted, where the dust plasma parameters are $\delta_1=2.5$. M and l_z have the same values as in Fig. 1. Two values of β are β=0.3,0.4. Here the dotted curve corresponds to β=0.4 and the solid curve is obtained for β=0.3.

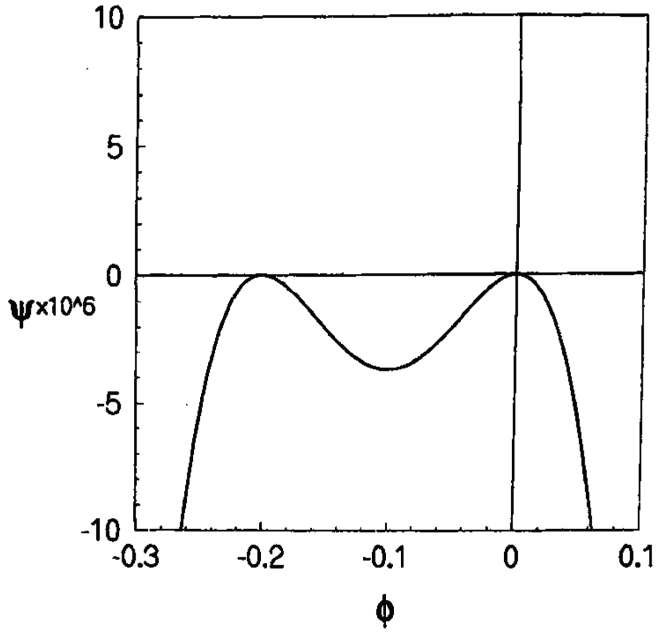

FIG. 9. Sagdeev's potential $\Psi=\psi*10^6$ vs ϕ is plotted, where the dust plasma parameters are $\delta_1=9.968$, $M=0.2$, $\beta=0.908$, $l_z=0.02$.

$=\frac{9}{2}A_1A_3$ which occurs in the case of the double layer solitary wave. Figure 10 shows the potential profile obtained by using the expression for ϕ given in Eq. (43).

Mamun *et al.*[18] considered a different plasma model and showed that the soliton amplitude is independent of the external magnetic field. Contrary to this, we find that the amplitude depends on the external magnetic field. However, Mamun *et al.* considered a different plasma model without assuming quasineutrality. We have found the respective ranges of various parameters for which solitary waves and double layers exist. From Eq. (36), (37), and (41) it is seen that a_1, a_2, a_3 depend on the values of β. So the amplitude of solitary wave changes as the value of external magnetic field changes. To conclude we have studied ion-acoustic solitary waves in a magnetized dusty plasma comprising Boltzmann distributed electrons, ions and dust grains and found out the respective ranges of physical parameters for which solitary waves and shock waves would exist. It is also shown that these ranges differs from the case when quasineutrality is assumed. Also we found that the higher order solution is important as it gives an idea how much effect higher order

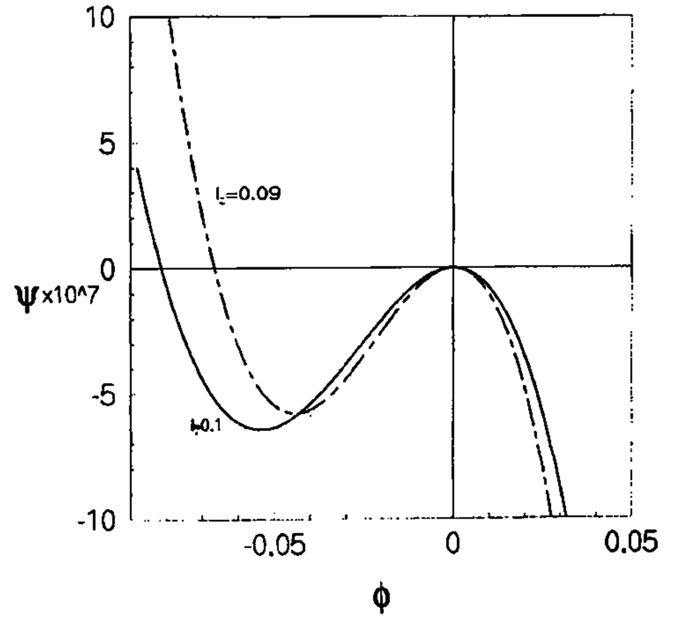

FIG. 8. $\Psi=\psi*10^7$ vs ϕ is plotted, where the dust plasma parameters are $\delta_1=2.5$, $M=0.2$, $\beta=0.48$. The two values l_z used are l_z=0.1,0.09. Here the solid curve corresponds to $l_z=0.1$ and the dotted one is obtained for $l_z=0.09$.

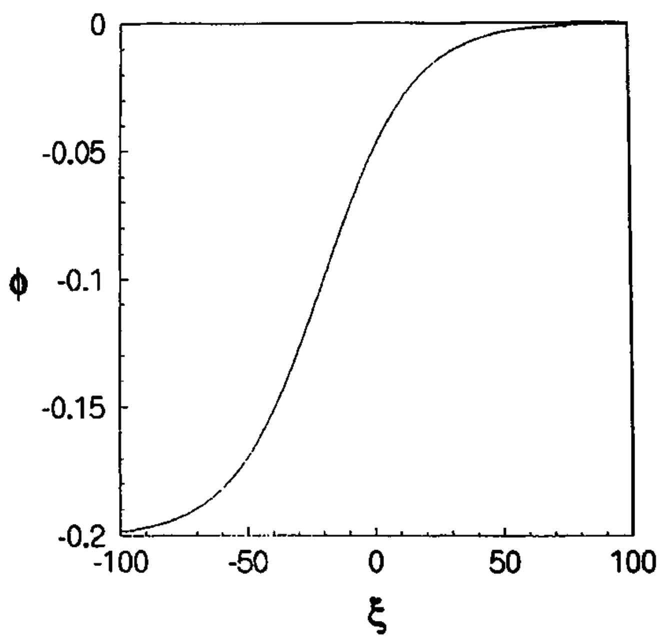

FIG. 10. ϕ vs ξ is plotted using the expression (43) with $\delta_1=9.968$, where other parameters are the same as those used in Fig. 9.

terms have and also provides justification for truncating the series for example, as was done in Eq. (39).

APPENDIX

$$A=\frac{1}{l_x}\left[-\frac{l_z^2}{M}+2a_1M\right], \tag{A1}$$

$$B=\frac{1}{l_x}\left[-\frac{l_z^2a_1}{M}+3a_2M-4a_1^2M\right], \tag{A2}$$

$$C=\frac{1}{l_x}\left[-\frac{l_z^2a_2}{M}+4Ma_3-12a_1a_2M+8a_1^3M\right], \tag{A3}$$

$$D=\frac{1}{l_x}\left[-\frac{l_z^2a_3}{M}+5a_4M-16a_1a_3M-9a_2^2M+36a_1^2a_2M-16a_1^4M\right], \tag{A4}$$

$$X_1=\frac{4\beta M^2}{l_x^2+l_z^2}, \tag{A5}$$

$$Y_1=\frac{\beta M(l_x-AM)}{l_x^2+l_z^2}, \tag{A6}$$

$$Z_1=\frac{1}{l_x}\left(\frac{l_z^2a_1}{M}+4a_1^2M\right), \tag{A7}$$

$$X_2=1+\frac{4\beta M^2}{l_x^2+l_z^2}(1-2\delta_1a_1), \tag{A8}$$

$$X_3=C-2Ba_1-3Aa_2-\frac{X_1}{4}\left(\frac{1}{2}-3\delta_1a_2\right)(2B-2Aa_1)+\frac{Y_1}{6}+Y_2+Y_3, \tag{A9}$$

$$Y_2=\frac{X_1}{4}\left[\left(\frac{1}{3}-2\delta_1a_2\right)2Aa_1+(1-2\delta_1a_1)(4Ba_1+6Aa_2-8Aa_1^2)\right], \tag{A10}$$

$$Y_3=-\frac{X_1}{4}\left[(1-2\delta_1a_1)(6C-4Ba_1)+2B\left(\frac{1}{3}-2\delta_1a_2\right)\right]. \tag{A11}$$

[1] P. K. Shukla, Phys. Plasmas 8, 1791 (2001).
[2] N. N. Rao, P. K. Shukla, and M. Y. Yu, Planet. Space Sci. 38, 543 (1990).
[3] P. K. Shukla and V. P. Silin, Phys. Scr. 45, 508 (1992).
[4] P. K. Shukla and H. U. Rahaman, Planet. Space Sci. 46, 541 (1998).
[5] P. K. Shukla, M. Y. Yu, and R. Bharuthram, J. Geophys. Res. 96, 21343 (1991).
[6] A. Barkan, R. L. Merlino, and N. D'Angelo, Phys. Plasmas 2, 3563 (1995).
[7] A. Thompson, A. Barkan, N. D'Angelo, and R. L. Merlino, Phys. Plasmas 4, 2331 (1997).
[8] Y. Nakamura and A. Sarma, Phys. Plasmas 8, 3921 (2001).
[9] P. K. Shukla and F. Verheest, Astron. Astrophys. 401, 849 (2003).
[10] P. Meuris and F. Verheest, Phys. Lett. A 219, 299 (1996).
[11] M. Ansar Mahmood, A. M. Mirza, P. H. Sakanaka, and G. Murtaza, Phys. Plasmas 9, 3794 (2002).
[12] O. A. Pokhotelov, O. G. Onishchenko, P. K. Shukla, and L. Stenlfo, J. Geophys. Res. 104, 19797 (1999).
[13] C. Yinhua and M. Y. Yu, Phys. Scr. 50, 298 (1994).
[14] K. D. Tripathi and S. K. Sharma, Phys. Rev. E 53, 1035 (1996).
[15] C. R. Choi, C. M. Ryu, N. C. Lee, and D. Y. Lee, Phys. Plasmas 12, 022304 (2005).
[16] C. R. Choi, C.-M. Ryu, N. C. Lee, D.-Y. Lee, and Y. Kim, Phys. Plasmas 12, 073301 (2005).
[17] R. Z. Sagdeev, *Reviews of Plasma Physics* (Consultants Bureau, New York, 1966), Vol. 4, p. 23.
[18] A. A. Mamun, P. K. Shukla, and L. Stenflo, Phys. Plasmas 9, 1474 (2002).
[19] V. P. Bhatnagar, G. Vanoost, A. M. Messisen, and P. E. Vandarplas, Plasma Phys. 18, 525 (1976).